Crystallographic Analysis of the Binding Modes of Thiazoloisoindolinone Non-Nucleoside Inhibitors to HIV-1 Reverse Transcriptase and Comparison with Modeling Studies

Jingshan Ren,[§] Robert M. Esnouf,[§,†] Andrew L. Hopkins,[§] David I. Stuart,*[,§,†] and David K. Stammers*[,§]

Laboratory of Molecular Biophysics, Rex Richards Building, South Parks Road, Oxford OX1 3QU, U.K., and Oxford Centre for Molecular Sciences, New Chemistry Building, South Parks Road, Oxford OX1 3QT, U.K.

Received June 3, 1999

We have determined the crystal structures of thiazoloisoindolinone non-nucleoside inhibitors in complex with HIV-1 reverse transcriptase to high-resolution limits of 2.7 Å (BM +21.1326) and 2.52 Å (BM +50.0934). We find that the binding modes of this series of inhibitors closely resemble that of "two-ring" non-nucleoside reverse transcriptase inhibitors. The structures allow rationalization of stereochemical requirements, structure−activity data, and drug resistance data. Comparisons with our previous structures suggest modifications to the inhibitors that might improve resilience to drug-resistant mutant forms of reverse transcriptase. Comparison with earlier modeling studies reveals that the predicted overlap of thiazoloisoindolinones with TIBO was largely correct, while that with nevirapine was significantly different.

Introduction

Targeting the virally encoded reverse transcriptase (RT) has proved a successful strategy in the development of the drugs used to treat HIV infection and AIDS. The nucleoside analogue RT inhibitors (NRTIs), e.g. AZT, ddI, ddC, 3TC, d4T, are widely used anti-HIV drugs. The non-nucleoside reverse transcriptase inhibitors (NNRTIs) are now playing an increasingly important role in HIV chemotherapy. NNRTIs are generally specific for HIV-1 RT and have a non-competitive inhibition mode with respect to substrates.[1] X-ray crystallographic studies provide a structural rationalization for this inhibition mode, revealing a binding site for NNRTIs some 10 Å from the polymerase active site, within the p66 subunit of the p66/p51 heterodimer.[2−4] The mechanism of inhibition has been shown to be via a distortion of the conformation of the catalytic aspartyl residues in the polymerase active site.[5] NNRTIs are generally lipophilic molecules, but otherwise are chemically diverse, and yet have been shown to have similar binding modes to HIV-1 RT.[3,4,6−9]

NNRTIs give rapid selection of resistant virus both in tissue culture and in clinical trials as monotherapy,[10,11] but there is now considerable interest in this class of inhibitor when used as multidrug therapy in combination with other anti-RT drugs and HIV protease inhibitors. To date, three NNRTI drugs have been licensed for clinical use: nevirapine, delavirdine, and efavirenz. Efavirenz together with certain carboxanilides and quinoxalines have been classed as "second-generation" NNRTIs, because of much-improved resilience to the effects of some of the common drug-resistance mutations.[1] The emerging therapeutic role for NNRTIs has led to a recrudescence of interest in developing further drugs in this class, but with improved potency and resistance profiles. To assist such drug design efforts, three-dimensional structures have been determined for members of several NNRTI series in complex with HIV-1 RT.[2−4,6−9] However, for technical reasons, the number of HIV RT/NNRTI crystal structures available is significantly less than for the much simpler HIV protease inhibitor complexes. An alternative approach to understanding drug/receptor interactions, in the absence of experimentally determined structures, is to deduce information on the nature of such interactions by molecular modeling studies. Such predictions can obviously be tested when subsequent structure determinations allow comparison of modeled and experimental data. Crystal structures of RT/carboxanilide complexes,[9] for example, show that one modeling study deduced many correct features,[12] while a second had an incorrect *trans* conformation for the inhibitor,[13] thereby leading to largely erroneous predictions for the interactions of the compound with the protein.

A series of thiazoloisoindolinone NNRTI compounds have been described,[14] which show potent HIV inhibition (IC_{50} of 16 nM for the most potent compound). There is, however, a significant decrease in activity for such compounds in the presence of the common NNRTI-resistance mutation Tyr181Cys.[15] A computational study, carried out on these inhibitors prior to the availability of RT/NNRTI structures, used small molecule crystal structures of various inhibitors for molecular orbital calculations. These MNDO (modified neglect of diatomic differential overlap) maps were in turn used to generate overlaps with two NNRTIs, nevirapine and TIBO. This study allowed predictions for thiazoloisoindolinone conformations and orientations at the drug binding site.[16]

We have now determined the structures of HIV-1 RT complexes with two such thiazoloisoindolinones, BM +21.1326 ((*R*)−(+)-9b-(3-methylphenyl)-2,3-dihydrothiazolo[2,3-*a*]isoindol-5(9b*H*)-one) and BM +50.0934 ((*R*)−(+)-5(9b*H*)-oxo-9b-phenyl-2,3-dihydrothiazolo[2,3-*a*]isoindole-3-carboxylic acid methyl ester), by X-ray crystallography to 2.7 and 2.52 Å resolution, respectively.

* Corresponding authors.
[§] Laboratory of Molecular Biophysics.
[†] Oxford Centre for Molecular Sciences.

10.1021/jm990275t CCC: $18.00
Published on Web 09/03/1999

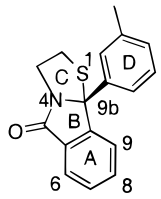

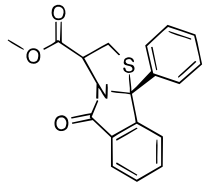

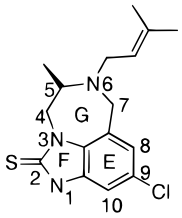

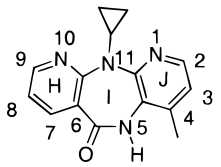

These refined crystal structures reveal a detailed picture of both the RT-bound drug conformations and the interactions of the drugs with their receptor. This allows comparison with earlier modeling studies, rationalization of structure−activity data, and drug-resistance data, as well as allowing us to suggest alterations to these compounds that might improve their resistance profiles.

Results and Discussion

Comparison of Conformations for Thiazoloisoindolinones and Other NNRTIs. Electron density maps for the complexes reveal that BM +21.1326 and BM +50.0934 are bound at the NNRTI site (Figure 1). A comparison of the conformations of BM +21.1326, nevirapine, and Cl-TIBO when bound to HIV-1 RT is shown in Figure 2a. The conformation of BM +50.0934 is largely similar to that of BM +21.1326 apart from a slight displacement of the D phenyl ring due the absence of the *m*-methyl substituent. The inhibitors conform to the "two-ring" bound NNRTI conformation previously noted.[3,6] Thus, ring A of BM +21.1326 overlaps with the H ring of nevirapine, while the *m*-methylphenyl ring (ring D) partially overlaps the J ring of nevirapine. The comparable overlaps for Cl-TIBO involve the tricyclic ring system (rings E, F, G) with the isoindolinone (rings A, B) of BM +21.1326 and BM +50.0934 and the dimethylallyl group of Cl-TIBO with the D rings of the thiazoloisoindolinone compounds.

The thiazolo ring (ring C) overlaps with the cyclopropyl group of nevirapine and provides the means to flip the side chain of Tyr181 into the 'up' position, presumably giving tight binding in an analogous way to that previously noted for certain HEPT analogues.[7]

We have compared the crystallographic results for thiazoloisoindolinones bound to RT with the previous modeling work reported by Schafer et al.[16] Compound overlaps from both experimentally determined and modeling work are shown in Figure 2. These reveal that the modeled overlap of BM +21.1326 with Cl-TIBO is essentially correct except that this places the rather flexible dimethylallyl group of Cl-TIBO too far away from the phenyl ring (ring D) of BM +21.1326.

In contrast, the modeled overlap of BM +21.1326 with nevirapine is not entirely correct. The pseudo-chiral 11-position nitrogen of nevirapine gives rise to two conformations for this drug, both of which are observed in the small molecule crystal of the inhibitor.[17] Unfortunately, Schafer et al.[16] based their analysis on one nevirapine conformer which was later shown to be the one not bound to RT.[2,3] The incorrect choice of nevirapine conformation means that the nevirapine fused-ring system is bent in the opposite sense and thus requires a 180° flip to overlap with BM +21.1326. However, due to the pseudo-symmetric nature of these drug molecules,[3] the resulting overlaps still have rings A and H as well as rings D and J congruent, albeit with the direction of, for example, the *m*-substituent of BM +21.1326 reversed in direction. As a result, possible overlaps in substituents between nevirapine and the thiazoloisoindolinone were incorrectly inferred.

Interactions of Thiazoloisoindolinone with RT and Effects of Drug-Resistance Mutations. BM +21.1326 makes many interactions with HIV-1 RT that are commonly observed for other NNRTIs, with most of the contacts being hydrophobic in nature. There are extensive interactions of the D ring with Tyr188, as well as with other aromatic residues including Trp229 and Tyr318 involving both A and B rings. Other interactions are with Leu100, Lys101, Lys103, Val106, and Val179 (see Figure 3). BM +50.0934 lacks the *m*-methyl substituent of the D ring, which results in a slight repositioning of this ring. This, in turn, gives closer interactions with the side chain of Tyr181. A further difference between BM +21.1326 and BM +50.0934 is the presence of a methoxymethanoyl ester substituent on the C ring. This group makes contacts with Glu138 from the p51 subunit, as well as with the protein backbone of Ile180 and Tyr181 of the p66 subunit.

HIV-resistance data have been reported for two members of the thiazoloisoindolinone series,[15] BM +21.1298 and BM +51.0836 which differ from BM +21.1326 by their substituent pattern in the D ring. BM +21.1298 lacks the *m*-methyl group, while BM +51.0836 has *m*-dimethyl substituents. These two thiazoloisoindolinones were tested in serial passaging experiments with HIV-1 in tissue culture. Escape mutants identified from this study showed the change of Tyr181Cys, which is among the most commonly found mutations giving resistance to NNRTIs.[18] Inhibition data for mutant RTs show that the Tyr181Cys mutation gives a 30− 60-fold increase in IC_{50} for these thiazoloisoindolinone compounds. Other mutations which confer cross-resistance to the thiazoloisoindolinones include Lys103Asn (60−120-fold), Lys101Ala (40−60-fold), and Tyr188Leu (70−100-fold).[15] Analysis of our RT/thiazoloisoindolinone structures helps rationalize some of these resistance data. There are a number of van der Waals contacts between both the thiazoloisoindolinones and Tyr188; hence a mutation at this residue potentially gives a large loss of binding. In the case of Tyr181, BM +50.0934 makes close contacts, while BM +21.1326 is positioned slightly further away, the substitution pattern on the D ring appearing to modulate this interaction. For Lys103 there are contacts for both BM +21.1326 and BM +50.0934 with the $C\epsilon$ and $C\gamma$ atoms of the side chain via the B ring oxygen atom, and hence shortening of the side chain to Asn is likely to reduce these interactions.

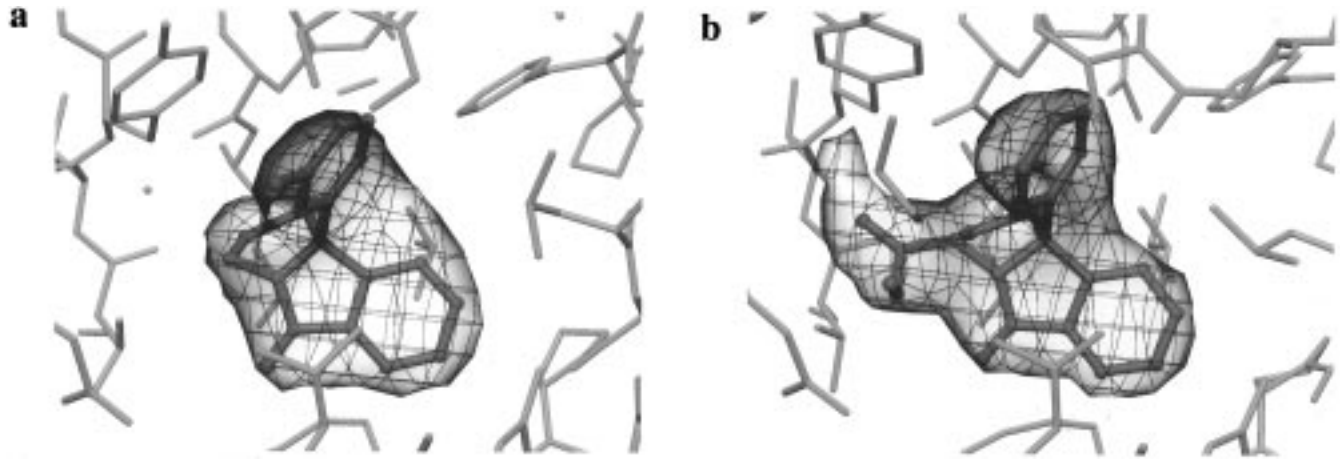

Figure 1. Simulated annealing omit electron density maps showing the bound inhibitors in the NNRTI pocket of HIV-1 RT: (a) BM +21.1326; (b) BM +50.0934. The maps are contoured at 3σ.

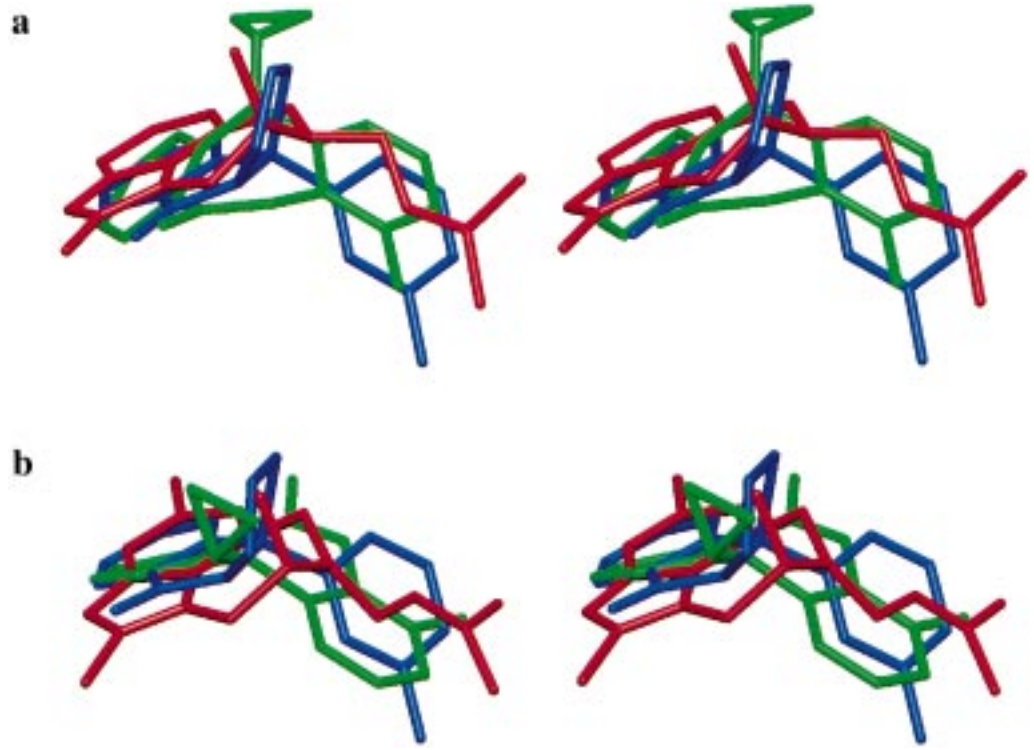

Figure 2. Stereodiagram showing the relative orientations and positions of nevirapine (green), TIBO (red), and BM +21.1326 (blue) from (a) experimental results reported here and (b) modeling.[16] The superimposition for panel a was done as described previously.[3]

Rationalization of Structure−Activity Data and Design of New Inhibitors. A number of analogues of the thiazoloisoindolinones have been synthesized and structure−activity studies reported.[14] The effects of differing substituent patterns of the C, D, and A rings can be viewed in the context of our structural results (Figure 4). Variations in the D ring show that there are both bulk and hydrophobicity restrictions. Five-membered rings such as furanyl and pyrrolyl lose activity as they not only are more hydrophilic than phenyl groups but also make less contacts with the side chains of Trp229, Tyr188, and Tyr181. More hydrophilic six-membered D rings such as pyridinyl or pyrimidinyl also show lower potency than the corresponding phenyl rings. With a phenyl group as the D ring, a *m*-methyl substituent makes contacts with the side chain of Trp229, giving rise to a 20-fold increase in binding. However, a *m*-dimethylphenyl D ring appears to fill this pocket optimally, making good contacts with the indole ring of Trp229, and is the most potent in the series. In contrast, the *m*,*p*-dimethyl substitution pattern does not fit as well, and neither do compounds with dichloro substituents. The presence of a *m*-methoxy substituent reduces activity due to both a greater bulk and to the introduction of more hydrophilicity in an otherwise hydrophobic pocket.

In the case of variants of the C ring, expansion to a six-membered ring reduces potency, due to bad contacts with the Cβ of Tyr188, as well with the side chain of Val179. Substituents at the C ring 1-position (also referred to as the 'X'-position[16]) give similar steric clashes. Part of ring C (R4-position) points to a more open region of the pocket, and thus, a bulky substituent such as the methoxymethanoyl group of BM +50.0934

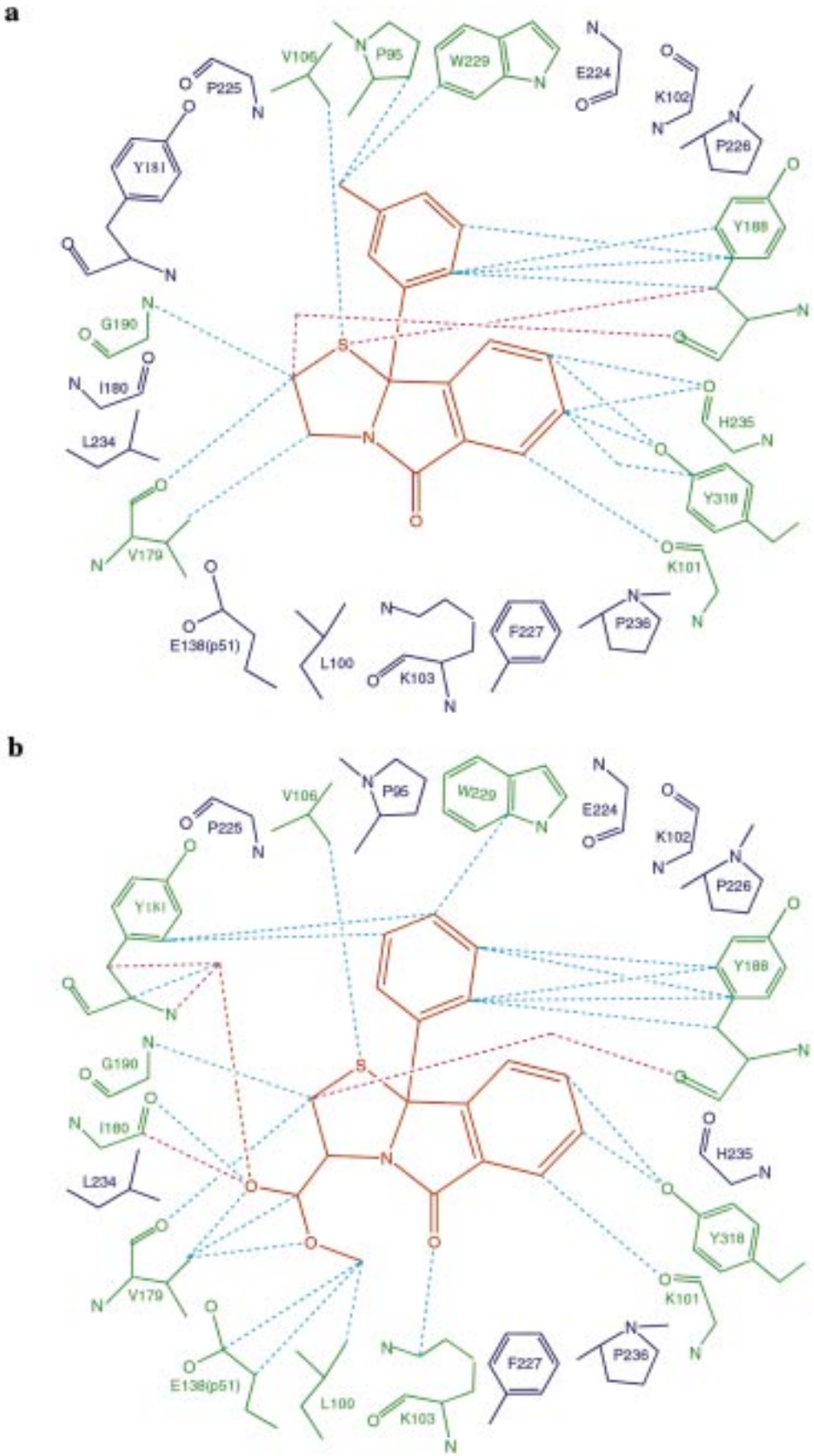

Figure 3. Schematic diagrams showing the intermolecular interactions between the thiazoloisoindolinone NNRTIs (in red) and the surrounding residues of HIV-1 RT for (a) BM +21.1326 and (b) BM +50.0934. Residues which contact the NNRTI with a minimum interatomic distance of <3.6 Å are shown in green, while other residues lining the binding pocket are shown in blue. The individual distances between the NNRTI and the protein atoms are shown as dashed lines (distances < 3.3 Å in pink; 3.3 Å < distances < 3.6 Å in light blue).

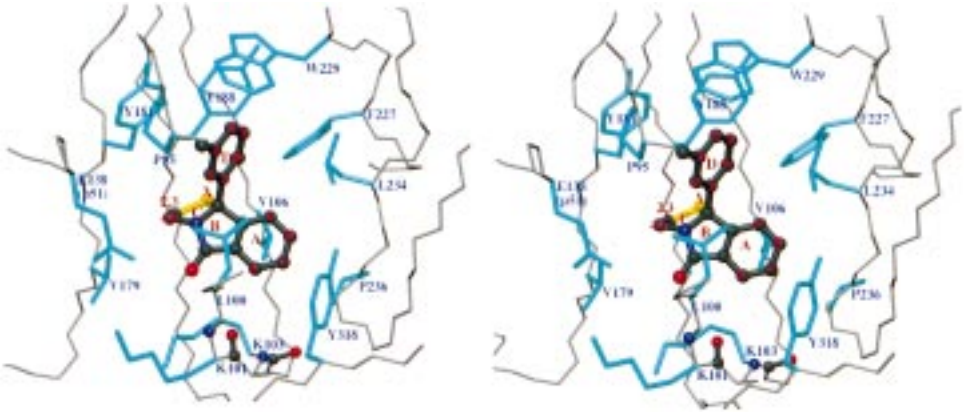

Figure 4. Stereoview of BM +21.1326 positioned in the NNRTI binding pocket. RT side chains that form the NNRTI binding site are marked, together with substituent positions as described by Mertens et al.[14] For clarity the *R*2,3- and *R*4,5-positions of the C ring are labeled 2,3 and 4,5, respectively.

Table 1. Statistics for Crystallographic Structure Determinations

	RT/BM +21.1326	RT/BM +50.0934
data collection details:		
data collection site	ID2, ESRF	BL14, ESRF
wavelength (Å)	0.995	0.930
collimation (mm)	0.05 × 0.05	0.21 × 0.22
crystal form	G	E
unit cell (*a*, *b*, *c* in Å)	135.1, 112.7, 75.1	137.3, 108.5, 72.0
resolution range (Å)	20.0−2.70	15.0−2.52
observations	64045	115112
unique reflections	26072	32729
completeness (%)	81.2	88.8
reflections with $F/\sigma(F) > 3$	23500	28620
R_{merge} (%)[a]	6.7	8.7
outer resolution shell:		
resolution range (Å)	2.80−2.70	2.62−2.52
unique reflections	2114	2708
completeness (%)	64.7	64.5
reflections with $F/\sigma(F) > 3$	1364	1631
refinement statistics:		
resolution range (Å)	20.0−2.70	15.0−2.52
unique reflections (working/test)	26072 (24813/1259)	32729 (31104/1625)
R-factor[b] (*R*-working/*R*-free)	0.214/0.276	0.232/0.298
number of atoms[c]	7103/43/20	7824/90/23
rms bond length deviation (Å)	0.008	0.007
rms bond angle deviation (deg)	1.4	1.4
mean *B*-factor (Å^2)[d]	57/62/44/44	52/56/42/47
rms backbone *B*-factor deviation[e]	3.6	3.9

[a] $R_{merge} = \sum|I - \langle I\rangle|/\sum\langle I\rangle$. [b] *R*-factor $= \sum|F_o - F_c|/\sum F_o$. [c] Protein atoms/water molecules/inhibitor atoms. In the RT/BM +21.1326 complex, due to the crystal packing, residues 1−3, 28−44, 49−53, 63−72, and 131−143 are disordered in the p66 fingers domain; residues 539−560 of the p66 subunit, as well as residues 1−5, 88−95, 191−232 and 428−440 of the p51 subunit, are also not defined in the electron density map. Residues 444−454 of the RNase H domain in this crystal form are ordered, as observed in crystal forms C and E,[3,5] while the C-terminal end of p51 chain is disordered, similar to crystal forms D and F.[3,6] In the RT/BM +50.0934 complex, residues 540−560 of the p66 and residues 88−92 and 216−231 have been omitted from the model. [d] Mean *B*-factor for main-chain, side-chain, water, and inhibitor atoms, respectively. [e] rms deviation between *B*-factors for bonded main-chain atoms.

can be accommodated and, indeed, is able to form favorable interactions with Glu138 resulting in a 3-fold greater potency.

For modifications of the A ring, the 8-chloro substituent gives an 8-fold improvement in potency. This is positioned within the NNRTI pocket in a similar location to the equivalent atom of 8-Cl-TIBO and hence can make favorable van der Waals contacts with the protein main chain at residues 234 and 235. This similarity was correctly predicted by the modeling studies of Schafer et al.[16]

Knowledge of the RT binding mode for thiazoloisoindolinones reported here, together with our previous data on the binding of other NNRTIs to RT, allows suggestions for modifications to the compounds that could improve their properties. In our study of the carboxanilide NNRTI UC-781,[9] we identified a combination of structural factors that could contribute to the so-called "second-generation" NNRTI properties of resilience to common drug-resistant mutant RTs. These factors included small, non-aromatic substituents in the upper subpocket, main-chain hydrogen bonding, and optimal bulk within the pocket. Applying these factors to the thiazoloisoindolinones, the D ring could be replaced by an acyclic moiety such as a dimethylallyl group. The C ring could be dispensed with leaving, perhaps, an ethyl group in the place of the sulfur atom to enable the Tyr181 side chain to be correctly positioned for tight binding.[7] There appears to be two ways to incorporate hydrogen bonding to the main chain of Lys101. First replacement of the carbonyl oxygen of ring B by methyleneamino in order to form a hydrogen bond to the

main-chain oxygen of Lys101. Second, a substituent on the A ring, containing an acceptor such as a carbonyl oxygen, would allow hydrogen bonding to the main-chain NH of Lys101. It also appears possible to form hydrogen bonds from NNRTIs to the main chain of Lys103, as we have previously observed in the case of BHAP.[8]

Conclusions

The detailed description of the interaction of two members of the thiazoloisoindolinone series with HIV-1 RT adds further to an understanding of the characteristics of NNRTIs binding to their drug receptor site. These inhibitors bind in a mode resembling that of "two-ring" NNRTIs, and on the basis of this similarity, we can rationalize much of the structure−activity and resistance data at the molecular level. We are also able to make definite suggestions for modified isoindolinones with improved resilience to common resistance mutations. Reconsideration of earlier modeling studies of the bound inhibitor conformation shows that the overlap of the thiazoloisoindolinone with TIBO is largely correct: the ring systems agreeing well, while the more flexible portion of TIBO is unsurprisingly more divergent. The incorrectly modeled overlap of thiazoloisoindolinone with nevirapine is a result of the interconvertible conformers produced by the pseudo-chiral center at the N11-position nitrogen of nevirapine.

Flexibility of the inhibitor molecules adds to the problems of predicting binding features correctly. Nevirapine has two major conformations, and consideration of the wrong conformer was enough to defeat the analysis. Other inhibitors have more variability, and thus the bound conformation may not be that observed in a crystal of the inhibitor alone where packing forces can significantly distort the conformation. Detailed high-resolution analysis of an array of enzyme/inhibitor complexes is thus a vital tool for directing rational drug design efforts.

Experimental Section

Crystallization and Data Collection. The crystals of complexes of RT with BM +21.1326 and BM +50.0934 were grown and treated prior to data collection as described.[19] X-ray data were collected at ESRF, Grenoble, France, using 30-cm MAR Research imaging plates operated in 18-cm mode. Crystals were flash-cooled and maintained at 100 K during data collection. Data frames of 1.5° oscillations were collected with exposure times of 15 s for RT/BM +21.1326 and 90 s for RT/BM +50.0934. Indexing and integration of data images were carried out with DENZO, and data were merged with SCALEPACK.[20] The unit cell dimensions of the RT/BM +21.1326 crystal differed from those recorded before but are closest to the G crystal form.[21] A summary of the X-ray data statistics is given in Table 1.

Structure Solution and Refinement. The orientation and position of the molecule in the unit cell were determined using rigid-body refinement with XPLOR.[22] The RT/9-Cl-TIBO complex (1rev)[6] was used as an initial model for RT/BM +21.1326 and the RT/MKC-442 complex (1rt1)[7] for RT/BM +50.0934. The structures were first refined with XPLOR and then with CNS,[23] using positional, simulated annealing and individual *B*-factor refinement with bulk solvent correction and anisotropic *B*-factor scaling. The topolgy and parameter dictionaries used in the refinement for the two inhibitors were derived from the crystal structures of BM +21.1326.[16] Model rebuilding was done using FRODO[24] on an Evans and Sutherland ESV workstation. For RT/BM +21.1326, positional restraints were applied to all atoms distant from the NNRTI binding site (defined as greater than 25 Å from the Cα atom of residue 188) throughout the refinement due to the smaller number of observations.

The structure of RT/BM +21.1326 has been refined to an *R*-factor of 0.214 (*R*-free: 0.276) for all data in the range of 20.0−2.70 Å resolution with rms deviations for bond lengths and bond angles from canonical values of 0.008 Å and 1.4°, respectively. The corresponding figures for RT/BM +50.0934 are *R*-factor of 0.232 (*R*-free: 0.298) for all data in the range of 15.0−2.52 Å resolution with rms deviations of 0.007 Å and 1.4° from the canonical bond lengths and bond angles, respectively. Table 1 summarizes the statistics on X-ray data and model refinement.

The coordinates and structure factors for the RT/BM +21.1326 and RT/BM +50.0934 complexes will be deposited with the Protein Data Bank and are scheduled for release 1 year after publication (PDB ID codes 1c0t and 1c0u, respectively).

Acknowledgment. We thank the U.K. MRC for long-term funding of the RT work with grants to D.K.S. and D.I.S. We also thank Dr. W. Schafer of Boehringer-Mannheim for the gift of compounds BM +21.1326 and BM +50.0934 and for helpful discussions.

References

(1) De Clercq, E. The role of nonnucleoside reverse transcriptase inhibitors (NNRTIs) in the therapy of HIV-1 infection. *Antiviral Res.* **1998**, *38*, 153−179.
(2) Kohlstaedt, L. A.; Wang, J.; Friedman, J. M.; Rice, P. A.; Steitz, T. A. Crystal structure at 3.5 Å resolution of HIV-1 reverse transcriptase complexed with an inhibitor. *Science* **1992**, *256*, 1783−1790.
(3) Ren, J.; Esnouf, R.; Garman, E.; Somers, D.; Ross, C.; Kirby, I.; Keeling, J.; Darby, G.; Jones, Y.; Stuart, D.; Stammers, D. High-resolution structures of HIV-1 RT from four RT-inhibitor complexes. *Nature Struct. Biol.* **1995**, *2*, 293−302.
(4) Ding, J.; Das, K.; Tantillo, C.; Zhang, W.; Clark, A. D. J.; Jessen, S.; Lu, X.; Hsiou, Y.; Jacobo-Molina, A.; Andries, K.; Pauwels, R.; Moereels, H.; Koymans, L.; Janssen, P. A. J.; Smith, R. H. J.; Kroeger Koepke, R.; Michejda, C. J.; Hughes, S. H.; Arnold, E. Structure of HIV-1 reverse transcriptase in a complex with the nonnucleoside inhibitor α-APA R 95845 at 2.8 Å resolution. *Structure* **1995**, *3*, 365−379.
(5) Esnouf, R.; Ren, J.; Ross, C.; Jones, Y.; Stammers, D.; Stuart, D. Mechanism of inhibition of HIV-1 reverse transcriptase by nonnucleoside inhibitors. *Nature Struct. Biol.* **1995**, *2*, 303−308.
(6) Ren, J.; Esnouf, R.; Hopkins, A.; Ross, C.; Jones, Y.; Stammers, D.; Stuart, D. The structure of HIV-1 reverse transcriptase complexed with 9-chloro-TIBO: lessons for inhibitor design. *Structure* **1995**, *3*, 915−926.
(7) Hopkins, A. L.; Ren, J.; Esnouf, R. M.; Willcox, B. E.; Jones, E. Y.; Ross, C.; Miyasaka, T.; Walker, R. T.; Tanaka, H.; Stammers, D. K.; Stuart, D. I. Complexes of HIV-1 reverse transcriptase with inhibitors of the HEPT series reveal conformational changes relevant to the design of potent nonnucleoside inhibitors. *J. Med. Chem.* **1996**, *39*, 1589−1600.
(8) Esnouf, R. M.; Ren, J.; Hopkins, A. L.; Ross, C. K.; Jones, E. Y.; Stammers, D. K.; Stuart, D. I. Unique features in the structure of the complex between HIV-1 reverse transcriptase and the bis-(heteroaryl)piperazine (BHAP) U-90152 explain resistance mutations for this nonnucleoside inhibitor. *Proc. Natl. Acad. Sci. U.S.A.* **1997**, *94*, 3984−3989.
(9) Ren, J.; Esnouf, R. M.; Hopkins, A. L.; Warren, J.; Balzarini, J.; Stuart, D. I.; Stammers, D. K. Crystal structures of HIV-1 reverse transcriptase in complex with carboxanilide derivatives. *Biochemistry* **1998**, *37*, 14394−14403.
(10) Richman, D.; Shih, C.-K.; Lowy, I.; Rose, J.; Prodanovich, P.; Goff, S.; Griffin, J. Human immunodeficiency virus type 1 mutants resistant to nonnucleoside inhibitors of reverse transcriptase arise in tissue culture. *Proc. Natl. Acad. Sci. U.S.A.* **1991**, *88*, 11241−11245.
(11) Richman, D. D.; Havlir, D.; Corbeil, J.; Looney, D.; Ignacio, C.; Spector, S. A.; Sullivan, J.; Cheeseman, S.; Barringer, K.; Pauletti, D.; Shih, C.-K.; Myers, M.; Griffin, J. Nevirapine resistance mutations of human immunodeficiency virus type 1 selected during therapy. *J. Virol.* **1994**, *68*, 1660−1666.
(12) Esnouf, R. M.; Stuart, D. I.; De Clercq, E.; Schwartz, E.; Balzarini, J. Models which explain the inhibition of reverse transcriptase by HIV-1-specific (thio)carboxanilide derivatives. *Biochem. Biophys. Res. Commun.* **1997**, *234*, 458−464.

(13) Yang, S. S.; Pattabiraman, N.; Gussio, R.; Pallansch, L.; Buckheit, R. W. J.; Bader, J. P. Cross-resistance analysis and molecular modeling of nonnucleoside reverse transcriptase inhibitors targeting drug-resistance mutations in the reverse transcriptase of human immunodeficiency virus. *Leukemia* **1997**, *11*, 89−92.
(14) Mertens, A.; Zilch, H.; Konig, B.; Schafer, W.; Poll, T.; Kampe, W.; Seidel, H.; Leser, U.; Leinert, H. Selective nonnucleoside HIV-1 reverse transcriptase inhibitors. New 2,3-dihydrothiazolo-[2,3-a]-isoindol-5(9bH)-ones and related compounds with anti-HIV-1 activity. *J. Med. Chem.* **1993**, *36*, 2526−2535.
(15) Maass, G.; Immendoerfer, U.; Koenig, B.; Leser, U.; Mueller, B.; Goody, R.; Pfaff, E. Viral resistance to the thiazolo-iso-indolinones, a new class of nonnucleoside inhibitors of human immunodeficiency virus type 1 reverse transcriptase. *Antimicrob. Agents Chemother.* **1993**, *37*, 2612−2617.
(16) Schafer, W.; Friebe, W.-G.; Leinert, H.; Mertens, A.; Poll, T.; von der Saal, W.; Zilch, H.; Ziegler, M. L. Non-Nucleoside Inhibitors of HIV-1 Reverse Transcriptase: Molecular Modelling and X-ray Structure Investigations. *J. Med. Chem.* **1993**, *36*, 726−732.
(17) Mui, P. W.; Jacober, S. P.; Hargrave, K. D.; Adams, J. Crystal structure of nevirapine, a nonnucleoside inhibitor of HIV-1 reverse transcriptase, and computational alignment with a structurally diverse inhibitor. *J. Med. Chem.* **1992**, *35*, 201−202.
(18) Schinazi, R. F.; Larder, B. A.; Mellors, J. W. Mutations in retroviral genes associated with drug resistance. *Int. Antiviral News* **1997**, *5*, 129−135.
(19) Stammers, D. K.; Somers, D. O. N.; Ross, C. K.; Kirby, I.; Ray, P. H.; Wilson, J. E.; Norman, M.; Ren, J. S.; Esnouf, R. M.; Garman, E. F.; Jones, E. Y.; Stuart, D. I. Crystals of HIV-1 reverse transcriptase diffracting to 2.2 Å resolution. *J. Mol. Biol.* **1994**, *242*, 586−588.
(20) Otwinowski, Z.; Minor, W. Processing of X-ray diffraction data collected in oscillation mode. *Methods Enzymol.* **1996**, *276*, 307−326.
(21) Esnouf, R. M.; Ren, J.; Garman, E. F.; Somers, D. O. N.; Ross, C. K.; Jones, E. Y.; Stammers, D. K.; Stuart, D. I. Continuous and discontinuous changes in the unit cell of HIV-1 reverse transcriptase crystals on dehydration. *Acta Crystallogr.* **1998**, *D54*, 938−954.
(22) Brunger, A. T. *X-PLOR Manual*; Yale University Press: New Haven, CT, 1992.
(23) Brunger, A. T.; Adams, P. D.; Clore, G. M.; Delano, W. L.; Gros, P.; Grosse, K. R. W.; Jiang, J. S.; Kuszewski, J.; Nilges, M.; Pannu, N. S.; Read, R. J.; Rice, L. M.; Simonson, T.; Warren, G. L. Crystallography and NMR system: A new software suite for macromolecular structure determination. *Acta Crystallogr.* **1998**, *D54*, 905−921.
(24) Jones, T. A. Interactive computer graphics: FRODO. *Methods Enzymol.* **1985**, *115*, 157−171.

JM990275T